Journal of Neuroradiology 46 (2019) 367–372

Available online at ScienceDirect www.sciencedirect.com

Elsevier Masson France EM|consulte www.em-consulte.com

Original Article

Differentiation between glioblastomas and brain metastases and regarding their primary site of malignancy using dynamic susceptibility contrast MRI at 3T

Askaner K[a,*], Rydelius A[b], Engelholm S[c], Knutsson L[d,h], Lätt J[e], Abul-Kasim K[a], Sundgren PC[f,g]

[a] Centre for Medical Imaging and Physiology, SUS, Malmoe, Sweden
[b] Department of Neurology, Lund, Sweden
[c] Department of Oncology, Lund, Sweden
[d] Department of Medical Radiation Physics, Lund University, Lund, Sweden
[e] Centre for Medical Imaging and Physiology, SUS, Lund, Sweden
[f] Institution of Clinical Sciences, Lund University, Lund, Sweden
[g] Department of Radiology, University of Michigan, Ann Arbor, US
[h] Department of Radiology and Radiological Science, Johns Hopkins University, Baltimore, US

ARTICLE INFO

Article history:
Available online 30 October 2018

Keywords:
CNS
MRI
Perfusion
Brain
Glioblastoma
Metastasis

ABSTRACT

Background. – Differentiation between glioblastoma and brain metastasis may be challenging in conventional contrast-enhanced MRI.
Purpose. – To investigate if perfusion-weighted MRI is able to differentiate glioblastoma from metastasis and, as a second aim was to see if it was possible in the latter group, to predict the primary site of neoplasm.
Material and methods. – Hundred and fourteen patients with newly discovered tumor lesion (76 metastases and 38 glioblastomas) underwent conventional contrast-enhanced MRI including dynamic susceptibility contrast perfusion sequence. The calculated relative cerebral blood volumes were analyzed in the solid tumor area, peritumoral area, area adjacent to peritumoral area, and normal appearing white matter in contralateral semioval center. The Student *t*-test was used to detect statistically significant differences in relative cerebral blood volume between glioblastomas and metastases in the aforementioned areas. Furthermore, the metastasis group was divided in four sub groups (lung-, breast-, melanoma-, and gastrointestinal origin) and using one-way ANOVA test. *P*-values < 0.05 were considered significant.
Results. – Relative cerebral blood volume (rCBV) in the peritumoral edema was significantly higher in glioblastomas than in metastases (mean 3.2 ± 1.4 and mean 0.9 ± 0.7), respectively, ($P < 0.0001$). No significant differences in the solid tumor area or the area adjacent to edema were found, ($P = 0.28$ and 0.21 respectively). There were no significant differences among metastases in the four groups.
Conclusion. – It is possible to differentiate glioblastomas from metastases by measuring the CBV in the peritumoral edema.
It is not possible to differentiate between brain metastases from different primaries (lung-, breast-, melanoma or gastrointestinal) using CBV-measurements in the solid tumor area, peritumoral edema or area adjacent to edema.

Introduction

Glioblastoma (GB) and cerebral metastases are the most common brain tumors in adults. Conventional contrast-enhanced magnetic resonance imaging (CE-MRI) is often non-conclusive due to similarities in imaging characteristics and contrast-enhancement pattern between these entities, especially in solitary lesions in patients with no known prior malignancy. In one study of 181 individuals, almost 55 % had no known prior malignancy at the time of detection of Metastases [1].

In lesions with a peripheral ring enhancement, it is often impossible to differentiate between GB and Met from the morphologic images only. GBs may present with multifocal areas of enhance-

* Corresponding author at: Centre for Medical Imaging and Physiology, SUS, 214 01 Malmoe, Sweden
E-mail address: krister.askaner@med.lu.se (K. Askaner).

https://doi.org/10.1016/j.neurad.2018.09.006
0150-9861/

ment, thus simulate multiple Met. Cerebellar tumor-like lesions in an adult population are often interpreted as metastases. Cerebellar GBs are uncommon and seem to show different radiological features compared to supratentorial GB [2] Differentiation between primary and metastatic brain lesions is important for correct initial treatment due to differences in therapeutic strategy [3]. Advanced MRI-techniques such as dynamic susceptibility contrast MRI (DSC-MRI) may give further dynamic and physiological information in brain tumor behavior. DSC-MRI is a method that evaluates cerebral blood volume (CBV) in brain tissue and is thought to reflect tumor vascularity [4]. Earlier studies have shown good relationship between grade of neovascularization and level of relative cerebral blood volume (rCBV) [4–7].

Metastases are secondary implanted tumor cells which are believed to initially attach to vascular basement membrane in pre-existing vessels [8] and grow along those vessels by "hijacking" existing vasculature, a mechanism called co-option [9]. Brain metastases do not exhibit diffuse infiltrative growth pattern like GBs. The peritumoral edema is thus thought to be purely vasogenic in metastases [10].

In contrary, neovascularization in GB is predominantly based on angiogenic sprouting from pre-existing capillaries [11]. The peritumoral edema in GB is a combination of infiltrative tumor cells and vasogenic edema. Newly formed vessels in GBs exhibit uneven distribution with serpentine course and arterio-venous fistulas. They are also structurally abnormal [12]. Elevated CBV as a result of neovascularization and leaky vessel walls in the surrounding edema thus favor GB diagnosis [7,13–15], Fig. 1.

Peritumoral edema and contrast enhancement of brain tumors are both thought to be due to a breakdown of the blood-brain barrier (BBB). However, the exact mechanism by which these two phenomena occur is not completely understood [16].

Earlier studies are primarily focused in differentiating GB from metastases or low- vs high grade gliomas [3,5,6,13,15,17,18–20] and are thus not focused in comparison between metastases from different primary locations.

The aim of this study was to investigate if measurement of CBV in contrast enhancing tumor area, the peritumoral edema, and tissue in the proximity of the peritumoral edema, called the area adjacent to edema, could help in the early imaging stage to differentiate GB from metastases. The second aim was to investigate if CBV values, with the same premises, was possible differentiate between different metastases *P*, depending on the origin of primary malignancy.

Material and methods

Patients

This prospective study was approved by our local ethical committee (#2010/199). Patients who underwent computerized tomography (CT) that showed lesion(s) with characteristics compatible with glioblastoma (GB) or cerebral metastases were included for further investigation with MRI. All patients signed informed consent prior to the MRI study. Patients with a history of prior neurosurgery, chemotherapy or radiation therapy were excluded from further analysis related to this study. Patients with a final diagnose of GB or cerebral metastases were finally included. The patients were included during a 6 year period (2010–2015). Extended MRI examination including DSC-MRI were performed in 114 patients, 38 with GB (4 multifocal) and 76 with metastases. All but two patients (multiple metastases from known lung- and breast cancer) underwent partial or total surgical resection with accompanying histopathological diagnosis. The latter was considered as a reference.

Examination protocols

The study was performed on a 3T whole-body scanner (Magnetom TRIO, Siemens AG, Erlangen, Germany). Thirteen patients, from the metastasis group were examined on a 3T whole-body-scanner (Magnetom Skyra, Siemens AG, Erlangen, Germany). The protocol included, beside conventional MR imaging, the DSC-sequence: (gradient echo (GRE) EPI, TR 1400 ms, TE 32 ms, slice thickness 5 mm with 1.5 mm gap). After 10 sec delay, gadolinium contrast (Dotarem® 279.3 mg/mL) was administered at a rate of 5 mL/s and a total dose of 0.1 mmol/kg body weight. Fifty complete cycles with 19 slices each were acquired. Conventional MR imaging consisted of sagittal T1W, axial T2W, axial FLAIR, axial DWI, axial T1W ± gadolinium (gad) and, coronal T1W coronal post gad.

Data post processing

The DSC-MRI data were processed with advanced MRI perfusion software (Nordic ICE ver 2.3.12, 2011, Nordic Imaging Lab AS, Bergen, Norway). The post processing algorithm included correction of contrast media leakage during the first passage. The method to calculate leakage corrected rCBV uses a non-enhancing whole brain region to estimate and remove T1- or $T2^*$ based leakage effects. [21,22]. Anterior cerebral artery (ACA) was used for arterial input function (AIF). Regions of interest (ROIs) were carefully placed in the solid tumor area, the peritumoral edema, the area adjacent to edema, and in the normal appearing white matter (NAWM) in contralateral semioval center, respectively. To ensure correct positioning of the ROIs, we used enhanced T1-weighted and T2 FLAIR images to define borders between contrast-enhanced tumor area, peritumoral edema, and normal appearing parenchyma. The highest CBV values were chosen by placing multiple ROIs in the selected areas, Fig. 2. The contrast-enhanced T1- weighted images were also reviewed to avoid areas with large vessels, hemorrhage, cyst, and necrosis. ROIs with the highest CBV values were chosen in the three areas mentioned above. Finally, the rCBV ratio was calculated by dividing the three CBV values each with the CBV value of NAWM.

Statistical analysis

For statistical analysis, initially the patients were grouped according to prior tumor type: GB or metastasis. Statistical analysis using SPSS (version 19). Mean and standard deviation (SD) were analyzed with Student *t*-test to determine if there were statistically significant differences of rCBV parameters between GB and metastasis groups in the analyzed areas. The metastasis group was then divided in four subgroups according to the site of primary tumor (lung, breast, melanoma, and gastrointestinal) and analyzed with one-way ANOVA to determine differences of significance in rCBV. *P*-values of < 0.05 were considered statistically significant.

Results

Patient demographics and final diagnoses are summarized in Table 1. Lesion localizations are presented in Table 2.

Imaging findings

In the GB group 9 (24%) were solid, 12 (31%) were ring enhancing, and 17 (45%) showed inhomogeneous contrast enhancement with central necrosis. In the metastasis group 34 (45%) were solid, 26 (34%) were cystic, and 16 (21%) were partially cystic. The term ring enhancing is used when the tumor shows a pure cystic center with a peripheral contrast-enhancing rim. In the metastases group, 44 out of 76 (58%) lesions were solitary.

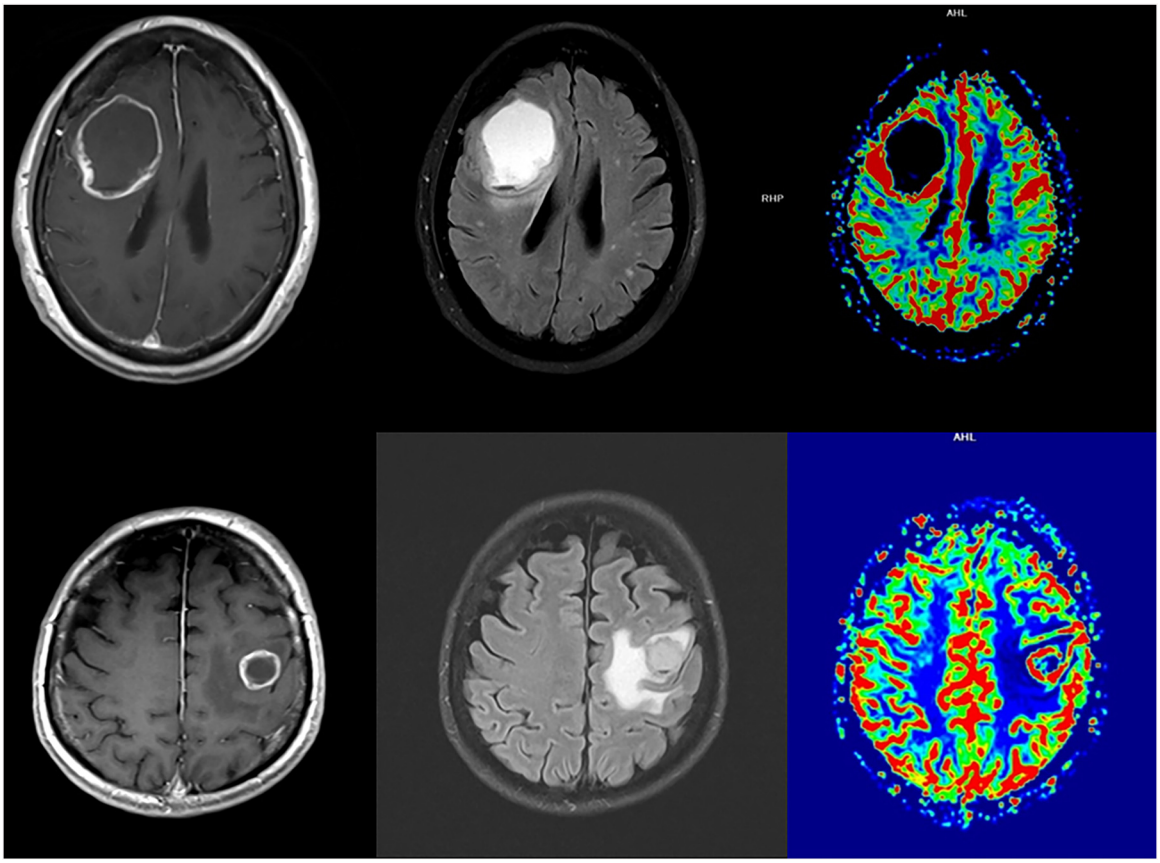

Fig. 1. Upper row from left, T1w + gad, T2 FLAIR and colored rCBV shows a cystic tumor with high rCBV in the peritumoral area consistent with GB. Lower row from left, T1w+ gad, T2 FLAIR and colored rCBV also shows a cystic tumor but with low rCBV in the peritumoral area consistent with a metastasis.

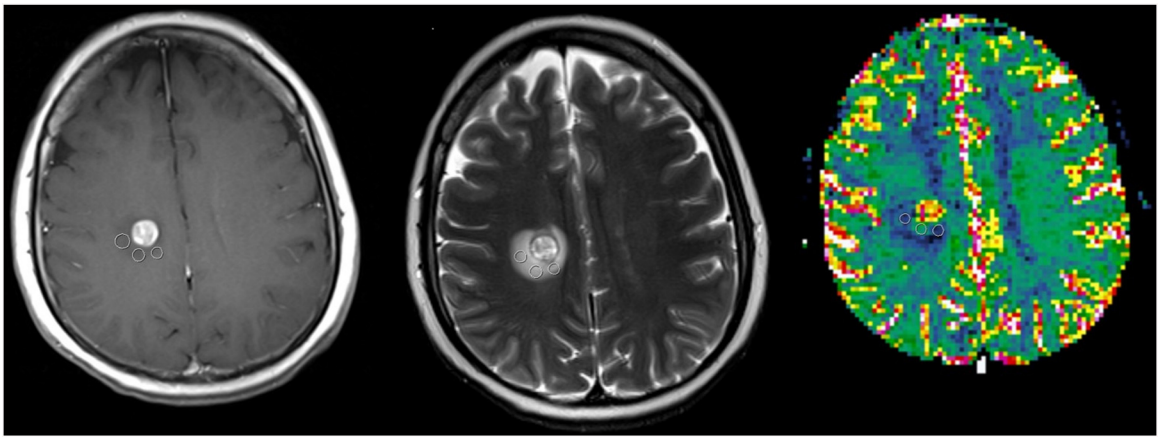

Fig. 2. Application of multiple ROI:s in the peritumoral edema to depict the highest rCBV-value. T1w + gad and T2w images are used in combination to avoid solid tumor area and include the peritumoral edema. From left to right, T1w + gad, T2w and colored rCBV images.

Table 1
Patient material.

Type	*n*	Age(range)	Age (mean)	Age (median)	Multifocal (GB)	Multiple metastases	Male/female %
GB	38	34–86	64	66	4		55/45
Metastasis (all)	76	31–91	64	67		32	40/60
Metastasis (lung)	32	49–82	67	69		15	42/58
Metastasis (melanoma)	12	43–77	63	64		5	73/27
Metastasis(breast)	12	31–73	56	55		5	0/100
Metastasis (GI)	10	48–77	64	64		3	40/60
Metastasis (other)[a]	10	40–91	67	70		4	40/60

GI: gastrointestinal.
[a] Includes metastases from kidney, cervix uteri, testis, ovary, prostate, and unknown primary.

Table 2
Location of GB and solitary Met from four major primary sites.

Location	GB ($n=38$)	Solitary Met all (n = 44)	Solitary Met lung ($n=17$)	Solitary Met breast ($n=7$)	Solitary Met melanoma ($n=7$)	Solitary Met GI ($n=7$)
Cerebrum	95%	33 (75%)	12 (70%)	4 (57%)	7 (100%)	4 (57%)
Cerebellum	5%	9 (20%)	4 (24%)	3 (43%)	0 (0%)	2 (29%)
Brainstem	0%	2 (5%)	1 (6%)	0 (0%)	0 (0%)	1 (14%)

GB: glioblastoma, Met: metastasis, GI: gastrointestinal.

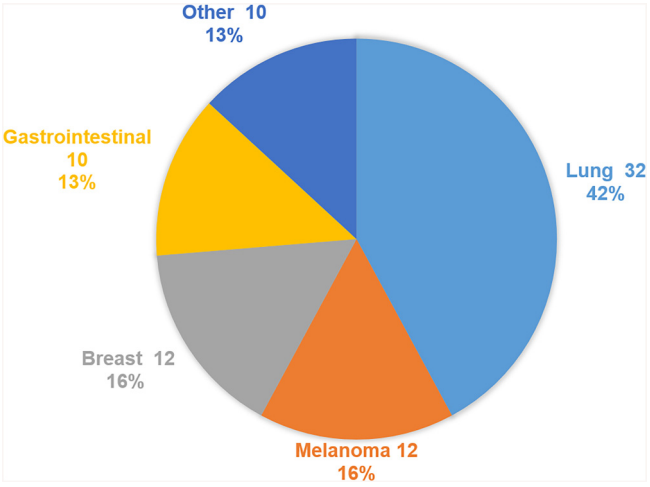

Fig. 3. Distribution of primary malignancy in the metastasis group.

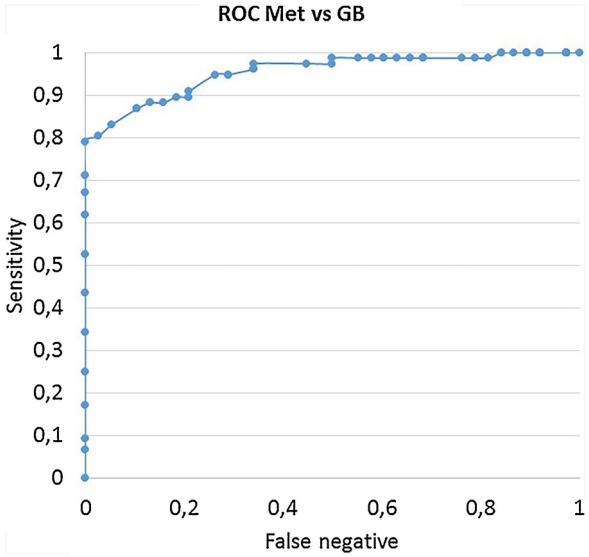

Fig. 4. ROC curve: Met vs GB, rCBV in the peritumoral edema.

Primary sites of metastases

In the metastases group, primary malignancy was unknown at the time of presentation in 24/76 patients (32%). In patients with solitary metastases, 16/44 (36%) had no known primary malignancy. After further investigations including histopathological evaluation, the metastases were distributed as follows, summarized in Fig. 3.

Solid tumor area

The mean rCBV ratio values in the solid tumor area in GB were $rCBV_{(GB\ ST)}$ 8.1 ± 3.6 and in metastases $rCBV_{(Met\ ST)}$ 7.0 ± 5.5. Comparing the rCBV ratios in the solid tumor area of GB with those of metastases showed no statistically significant difference, $P = 0.28$

Peritumoral edema

The mean rCBV ratio values in the peritumoral edema in GB were $rCBV_{(GB\ PTE)}$ 3.2 ± 1.4 and were significantly higher than those of metastases $rCBV_{(Met\ PTE)}$ 0.9 ± 0.71 ($P < 0.0001$).

Area adjacent to edema

The mean rCBV ratio values in the area adjacent to edema in GB were $rCBV_{(GB\ AAE)}$ 2.3 ± 1.2 and were not statistically different from those for metastases $rCBV_{(Met\ AAE)}$ 2.5 ± 1.7. ($P = 0.41$).

To define an optimal cut-off value a receiver operating characteristic (ROC) curve was made, Fig. 4. Using a cut-off value in $rCBV_{(met\ vs\ GB\ PTE)}$ of 1.1 yielded a sensitivity (sens), specificity (spec), negative predictive value (NPV), and positive predictive value (PPV) of 79%, 100%, 70%, and 100% respectively. Those cut-off values were chosen as all metastases showed a $rCBV \leq 1.1$ in the peritumoral area Cut-off value $rCBV_{(met\ vs\ GB\ PTE)}$ was 1.8, yielding a sens, spec, NPV, and PPV of 89%, 82%, 79%, and 91% respectively. Those cut-off values were derived from the ROC-curve.

Table 3
Previous studies and results regarding rCBV values in peritumoral area of GB and Met.

Study	GB	Met	rCBV GB	rCBV Met	Significance
Toh et al	$n=19$	$n=20$	1.62 ± 1.24	0.90 ± 0.35	$P=0.063$[a]
Chiang et al	$n=14$	$n=12$	2.33 ± 1.61	0.84 ± 0.33	$P<0.005$
Tsougos et al	$n=35$	$n=14$	1.68 ± 0.59	1.06 ± 0.38	$P=0.02$
Hakyemez et al	$n=22$	$n=26$	0.89 ± 0.51	0.33 ± 0.12	$P<0.001$
Law et al	$n=24$	$n=12$	1.21 ± 0.87	0.53 ± 0.12	$P<0.005$

GB = glioblastoma, Met = metastasis.
[a] Not statistically significant.

No significant differences were detected among the four groups of metastases (lung, breast, melanoma, and gastrointestinal tract) regarding values in solid tumor area, peritumoral edema or area adjacent to edema ($P = 0.97, 0.57, 0.86$ respectively).

Discussion

In our study, we found significant differences in rCBV regarding peritumoral edema in metastases versus GB. No differences were detected regarding solid tumor area or in area adjacent to the peritumoral edema. None of the aforementioned areas showed significant differences in rCBV between metastases with different primaries. Fifty-eight percent of the metastases were solitary when detected and 32 % of the patients in the metastatic group had no known prior malignancy at the time of presentation. This implies further the importance of differentiation between these entities due to different treatment schemes. Furthermore, there are different treatment schemes regarding solitary versus multiple metastases. Our results regarding differences in rCBV-values between glioblastomas and metastases in the peritumoral edema are consistent with earlier published results [3,14,15,18,23], Table 3. The novelty in our study is that we performed a systematic

comparison between brain metastases, with an aim to predict their primary malignancy. The number of individuals in the metastasis group in our study ($n = 76$) are significantly higher compared to most previous studies. Toh et al segmented the whole peritumoral edema instead of using multiple ROIs to depict the highest value. Since the peritumoral edema in GB is a mix of infiltrating tumor cells and vasogenic edema, it may have affected their results. Additionally, their study included solely thin rim-enhancing lesions. Earlier research have implied that thin rim-enhancing GB are associated with less peritumoral infiltration and higher survival rates [24]. Our study included in total 76 patients with metastases, based on the aim to differentiate metastases of different origin. Our and previous results are consistent with the fact that peritumoral edema in metastases represents pure vasogenic edema caused by plasma fluid leakage from nearby capillaries [25]. Additionally, it is proposed that decreased perfusion in the peritumoral edema in brain metastases is due to local compression of the microcirculation by the edema itself [26].

In agreement with earlier studies we found no differences between values in the solid tumor area of GB and metastases [3,14,15,18]. This implies the mechanism of high vascularity with leaky capillaries that demonstrate blood-brain-barrier breakdown in both GB and metastases. Interestingly, Toh et al showed statistically significant difference in CBV in the contrast-enhancing rim between thin rim-enhancing metastases and GB [23].

In addition to the aforementioned ROI areas, we also evaluated the area adjacent to the peritumoral area. The reason was to evaluate the hypothesis of tumor infiltration in GB beyond the visible edema in T2-weighted images. There were no statistically significant differences in the evaluated area between GB and metastases.

No differences were detected in the corresponding areas in metastases from the four different primary tumor sites. Gaudino et al had similar results in 59 patients with brain metastases [27]. This may be due to a similar mechanism in the pathogenesis of brain metastases regardless of origin [28]. The three metastasis groups in our study, beside the lung group ($n = 32$) were quite small ($n = 10–12$) which may have affected the result. We used the DSC technique to study brain perfusion as it is a fast robust technique relatively easy to post process and the most widely used technique especially in base line studies of brain tumors. Dynamic contrast-enhanced perfusion MRI (DCE-MRI) is more time consuming and requires more demanding post processing techniques. It is also very sensitive to signal to noise since there are a number of unknown parameters that needs to be fitted using different model approaches [29]. However, DCE-MRI may be a promising powerful tool in differentiating recurrent tumors from treatment related changes [30,31]. An additional aspect of DSC is to analyze the peak height (PH) and percentage of signal intensity recovery (PSR) of the initial signal curve derived from the first passage of contrast. This technique has described significant differences between GB and Met and is considered to depict differences in vascular permeability and neoangiogenesis [32,33]. Another recent study combined in a multiparametric fashion, PSR, PH, maximum rCBV and apparent diffusion coefficient (ADC) in differentiation of primary central nervous system lymphoma (PCNSL), metastases and GB where maximum rCBV in the peritumoral edema showed the strongest impact [34].

Other advanced MRI techniques, such as diffusion tensor- and kurtosis imaging (DTI, DKI) and MR-spectroscopy (MRS) have been used in earlier studies [3,14,27,35,36]. Bauer et al used a multiparametric approach that showed statistically significant differences between GB and metastases using a combination of CBV, fractional anisotropy (FA), and mean diffusivity (MD) in the peritumoral area. The combination yielded better significance than the individual techniques separately [37]. These results were based on a quite small group of 23 individuals (13 GB and 10 metastases). The results are though promising and needed to be validated in a larger cohort including MRS and DKI. In two recent articles, the use of computerized tomography perfusion (CTP) with promising results in differentiation of GB versus PCNSL and Met from different sites respectively [38,39]. The latter was a pilot study with a limited number of cases.

In conclusion, it is possible to differentiate glioblastomas from metastases by measuring

CBV in the peritumoral edema. All metastases showed an rCBV value in the peritumoral area less or equal to 1.1.

It is not possible to differentiate between brain metastases from different primaries (lung, breast, melanomas, and gastrointestinal) by CBV-measurements in the solid tumor area, peritumoral edema or in the area adjacent to edema.

Funding

This work was supported by Swedish Cancer Society [CAN 2013/321, CAN2016/365]; Swedish Research Council [VR K2011-52X-21737-01-3]; Malmö General Hospital Foundation for Fighting Against Cancer; ALF (Regional Research Funds) [F2014/354]; and Swedish Brain foundation [FO2014-0133].

Disclosure of interest

The authors declare that they have no competing interest.

References

[1] Giordana MT, Cordera S, Boghi A. Cerebral metastases as first symptom of cancer: a clinico-pathologic study. J Neurooncol 2000;50(3):265–73.
[2] Kikuchi K, Hiratsuka Y, Kohno S, Ohue S, Miki H, Mochizuki T. Radiological features of cerebellar glioblastoma. J Neuroradiol 2016;43(4):260–5.
[3] Chiang IC, Kuo Y-T, Lu C-Y, Yeung K-W, Lin W-C, Sheu F-O, et al. Distinction between high-grade gliomas and solitary metastases using peritumoral 3-T magnetic resonance spectroscopy, diffusion, and perfusion imagings. Neuroradiology 2004;46(8):619–27.
[4] Sugahara T, Korogi Y, Kochi M, Ikushima I, Hirai T, Okuda T, et al. Correlation of MR imaging-determined cerebral blood volume maps with histologic and angiographic determination of vascularity of gliomas. AJR Am J Roentgenol 1998;171(6):1479–86.
[5] Aronen HJ, Gazit IE, Louis DN, Buchbinder BR, Pardo FS, Weisskoff RM, et al. Cerebral blood volume maps of gliomas: comparison with tumor grade and histologic findings. Radiology 1994;191(1):41–51.
[6] Law M, Yang S, Babb JS, Knopp EA, Golfinos JG, Zagzag D, et al. Comparison of cerebral blood volume and vascular permeability from dynamic susceptibility contrast-enhanced perfusion MR imaging with glioma grade. AJNR Am J Neuroradiol 2004;25(5):746–55.
[7] Cha S. Neuroimaging in neuro-oncology. Neurotherapeutics 2009;6(3):465–77.
[8] Carbonell WS, Ansorge O, Sibson N, Muschel R. The vascular basement membrane as "soil" in brain metastasis. PLOS One 2009;4(6):e5857.
[9] Bugyik E, Dezso K, Reiniger L, László V, Tóvári J, Tímár J, et al. Lack of angiogenesis in experimental brain metastases. J Neuropathol Exp Neurol 2011;70(11):979–91.
[10] Pekmezci M, Perry A. Neuropathology of brain metastases. Surg Neurol Int 2013;4(Suppl 4):S245–55.
[11] Plate KH, Scholz A, Dumont DJ. Tumor angiogenesis and anti-angiogenic therapy in malignant gliomas revisited. Acta Neuropathol 2012;124(6):763–75.
[12] Nagy JA, Chang SH, Dvorak AM, Dvorak HF. Why are tumour blood vessels abnormal and why is it important to know? Br J Cancer 2009;100(6):865–9.
[13] Halshtok Neiman O, Sadetzki S, Chetrit A, Raskin S, Yaniv G, Hoffmann C. Perfusion-weighted imaging of peritumoral edema can aid in the differential diagnosis of glioblastoma mulltiforme versus brain metastasis. Isr Med Assoc J 2013;15(2):103–5.
[14] Tsougos I, Svolos P, Kousi E, Fountas K, Theodorou K, Fezoulidis I, et al. Differentiation of glioblastoma multiforme from metastatic brain tumor using proton magnetic resonance spectroscopy, diffusion and perfusion metrics at 3 T. Cancer Imaging 2012;26(12):423–36.
[15] Hakyemez B, Erdogan C, Gokalp G, Dusak A, Parlak M. Solitary metastases and high-grade gliomas: radiological differentiation by morphometric analysis and perfusion-weighted MRI. Clin Radiol 2010;65(1):15–20.
[16] Holodny AI, Nusbaum AO, Festa S, Pronin IN, Lee HJ, Kalnin AJ. Correlation between the degree of contrast enhancement and the volume of peritumoral edema in meningiomas and malignant gliomas. Neuroradiology 1999;41(11):820–5.
[17] Sparacia G, Gadde JA, Iaia A, Sparacia B, Midiri M. Usefulness of quantitative peritumoural perfusion and proton spectroscopic magnetic resonance imag-

ing evaluation in differentiating brain gliomas from solitary brain metastases. Neuroradiol J 2016;29(3):160–7.
[18] Law M, Cha S, Knopp EA, Johnson G, Arnett J, Litt AW. High-grade gliomas and solitary metastases: differentiation by using perfusion and proton spectroscopic MR imaging. Radiology 2002;222(3):715–21.
[19] Hakyemez B, Erdogan C, Bolca N, Yildirim N, Gokalp G, Parlak M. Evaluation of different cerebral mass lesions by perfusion-weighted MR imaging. J Magn Reson Imaging 2006;24(4):817–24.
[20] Cha S. Perfusion MR imaging of brain tumors. Top Magn Reson Imaging 2004;15(5):279–89.
[21] Bjornerud A, Sorensen AG, Mouridsen K, Emblem KE. T1- and T2*-dominant extravasation correction in DSC-MRI: part I – theoretical considerations and implications for assessment of tumor hemodynamic properties. J Cereb Blood Flow Metab 2011;31(10):2041–53.
[22] Boxerman JL, Schmainda KM, Weisskoff RM. Relative cerebral blood volume maps corrected for contrast agent extravasation significantly correlate with glioma tumor grade, whereas uncorrected maps do not. AJNR Am J Neuroradiol 2006;27(4):859–67.
[23] Toh CH, Wei K-C, Chang C-N, Ng S-H, Wong H-F, Lin C-P. Differentiation of brain abscesses from glioblastomas and metastatic brain tumors: comparisons of diagnostic performance of dynamic susceptibility contrast-enhanced perfusion MR imaging before and after mathematic contrast leakage correction. PLOS One 2014;9(10):e109172.
[24] Utsuki S, Oka H, Suzuki S, Shimizu S, Tanizaki Y, Kondo K, et al. Pathological and clinical features of cystic and noncystic glioblastomas. Brain Tumor Pathol 2006;23(1):29–34.
[25] Bertossi M, Virgintino D, Maiorano E, Occhiogrosso M, Roncali L. Ultrastructural and morphometric investigation of human brain capillaries in normal and peritumoral tissues. Ultrastruct Pathol 1997;21(1):41–9.
[26] Hossman KA, Bloink M. Blood flow and regulation of blood flow in experimental peritumoral edema. Stroke 1981;12(2):211–7.
[27] Gaudino S, Di Lella GM, Russo R, Lo Russo VS, Piludu F, Quaglio FR, et al. Magnetic resonance imaging of solitary brain metastases: main findings of non-morphological sequences. Radiol Med 2012;117(7):1225–41.
[28] Gavrilovic IT, Posner JB. Brain metastases: epidemiology and pathophysiology. J Neurooncol 2005;75(1):5–14.
[29] Jahng G-H, Li K-L, Ostergaard L, Calamante F. Perfusion magnetic resonance imaging: a comprehensive update on principles and techniques. Korean J Radiol 2014;15(5):554–77.
[30] Shin KE, Ahn KJ, Choi HS, Jung SL, Kim BS, Jeon SS, et al. DCE and DSC MR perfusion imaging in the differentiation of recurrent tumour from treatment-related changes in patients with glioma. Clin Radiol 2014;69(6):e264–72.
[31] Van Dijken BRJ, van Laar PJ, Holtman GA, van der Hoorn A. Diagnostic accuracy of magnetic resonance imaging techniques for treatment response evaluation in patients with high-grade glioma, a systematic review and meta-analysis. Eur Radiol 2017;27(10):4129–44.
[32] Cha S, Lupo JM, Chen MH, Lamborn KR, McDermott MW, Berger MS, et al. Differentiation of glioblastoma multiforme and single brain metastasis by peak height and percentage of signal intensity recovery derived from dynamic susceptibility-weighted contrast-enhanced perfusion MR imaging. AJNR Am J Neuroradiol 2007;28(6):1078–84.
[33] Chakravorty A, Steel T, Chaganti J. Accuracy of percentage of signal intensity recovery and relative cerebral blood volume derived from dynamic susceptibility-weighted, contrast-enhanced MRI in the preoperative diagnosis of cerebral tumours. Neuroradiol J 2015;28(6):574–83.
[34] Neska-Matuszewska M, Bladowska J, Sąsiadek M, Zimny A. Differentiation of glioblastoma multiforme, metastases and primary central nervous system lymphomas using multiparametric perfusion and diffusion MR imaging of a tumor core and a peritumoral zone-Searching for a practical approach. PLOS One 2018;13(1):e0191341.
[35] Steven AJ, Zhuo J, Melhem ER. Diffusion kurtosis imaging: an emerging technique for evaluating the microstructural environment of the brain. AJR Am J Roentgenol 2014;202(1):W26–33.
[36] Wang W, Steward CE, Desmond PM. Diffusion tensor imaging in glioblastoma multiforme and brain metastases: the role of p, q, L, and fractional anisotropy. AJNR Am J Neuroradiol 2009;30(1):203–8.
[37] Bauer AH, Erly W, Moser FG, Maya M, Nael K. Differentiation of solitary brain metastasis from glioblastoma multiforme: a predictive multiparametric approach using combined MR diffusion and perfusion. Neuroradiology 2015;57(7):697–703.
[38] Hiwatashi A, Togao O, Yamashita K, Kikuchi K, Yoshimoto K, Mizoguchi M, et al. Evaluation of glioblastomas and lymphomas with whole-brain CT perfusion: comparison between a delay-invariant singular-value decomposition algorithm and a Patlak plot. J Neuroradiol 2016;43(4):266–72.
[39] Dolgushin MB, Pronin IN, Holodny EA, Fadeeva LM, Holodny AI, Kornienko VN. Use of CT perfusion to discriminate between brain metastases from different primaries. Clin Imaging 2015;39(1):9–14.